Materials Characterization 136 (2018) 382–387

Contents lists available at ScienceDirect

Materials Characterization

journal homepage: www.elsevier.com/locate/matchar

High damping capacity of Al alloys produced by friction stir processing

C.Y. Liu[a,b,*], H.J. Jiang[a], B. Zhang[c], Z.Y. Ma[b,**]

[a] Key Laboratory of New Processing Technology for Nonferrous Metal & Materials, Ministry of Education, Guilin University of Technology, Guilin 541004, China
[b] Shenyang National Laboratory for Materials Science, Institute of Metal Research, Chinese Academy of Sciences, 72 Wenhua Road, Shenyang 110016, China
[c] State Key Laboratory of Metastable Materials Science and Technology, Yanshan University, Qinhuangdao 066004, China

ARTICLE INFO

Keywords:
Al alloy
Damping capacity
Fiction stir processing
Fine grain structure

ABSTRACT

Friction stir processing (FSP) was performed on both age-hardened and non-age-hardened Al alloys, with excellent damping properties obtained. The improved room temperature damping capacity of the FSP Al alloys can be mainly attributed to their low amount of solute atoms and the uniform distribution and high density of incoherent phases. The FSP Al alloys also exhibited improved high temperature damping capacity due to their equiaxed grain structure. The grain refinement and grain boundary pinning phase can further optimize the damping property of the FSP Al alloys. This work provides an effective strategy to improve the damping capacity of commercial Al alloys, which are regarded as low damping materials.

1. Introduction

Al alloys are vitally important structural materials due to their low density and excellent mechanical properties [1–3]. However, commercial Al alloys are regarded as low damping materials, which greatly limits their applications in some vibration sensitive equipment [4]. Thus, improving the damping capacity of commercial Al alloys is highly desirable to extend their engineering applications.

Macro-structure design, such as introducing a high density of macroscopic pores into Al matrixes to fabricate foamed Al [5] and friction stir welding (FSW) of high damping NiTi sheets with Al sheets to fabricate layered composites [6], can improve the damping capacity of Al products. However, macro-structure design does not change the physical properties of the matrix and is therefore not a fundamental method for improving the damping capacity of commercial Al alloys.

According to the Granato–Lücke model (dislocation damping mechanism) [7], controlling the presence and movement of movable dislocations can increase the room temperature damping capacity of metals. Crystal lattice defects, such as impurity atoms, vacancies, dislocation cells and walls can effectively pin the movable dislocations during vibration, and therefore deteriorate the room temperature damping capacity of metals [8]. However, the incoherent phases can increase the density of movable dislocations due to the mismatch in thermal expansion coefficients between these phases and the matrix, and therefore improve the room temperature damping capacity [9]. Thus, the room temperature damping capacities of commercial Al alloys are expected to improve by decreasing the dislocation pinning points and increasing the movable dislocations during vibration.

The dislocation damping mechanism is weakened by increased temperature. Luo et al. [10] found that the grain structures with excellent grain boundary (GB) sliding capacity always contributed to excellent high temperature damping capacity of metals. Therefore, the high temperature damping capacities of commercial Al alloys are expected to improve by enhancing the GB sliding capacity.

Commercial Al alloys after friction stir processing (FSP), which was developed based on the basic principles of FSW [11–14], showed excellent superplasticity when the deformation temperature was higher than 200 °C. This was attributed to their equiaxed fine grain structure that can lead to an excellent GB sliding behavior at high temperature [15–20]. Furthermore, other microstructural characteristics, which could improve the room temperature damping capacities of metals, such as the low density of dislocations and vacancies, low amount of solute atoms and uniform distribution of incoherent phases, were also obtained in FSP Al alloys [15–20]. Thus, FSP may be an effectively strategy to improve the damping capacity of commercial Al alloys.

In the present study, the effects of FSP with different rotation rates on the microstructure and damping capacity of the commercial age-hardened and non-age-hardened Al alloys are investigated. The aims are to fabricate Al alloys with excellent damping capacity and understand the key factors influencing the damping behavior of Al alloys.

* Correspondence to: C.Y. Liu, Key Laboratory of New Processing Technology for Nonferrous Metal & Materials, Ministry of Education, Guilin University of Technology, Guilin 541004, China.
** Corresponding author.
E-mail addresses: lcy261@glut.edu.cn (C.Y. Liu), zyma@imr.ac.cn (Z.Y. Ma).

https://doi.org/10.1016/j.matchar.2018.01.009
Received 15 November 2017; Received in revised form 31 December 2017; Accepted 5 January 2018
Available online 05 January 2018

Table 1
Parameters of each FSP sample. (LRR-FSP: FSP at low rotation rate; HRR-FSP: FSP at high rotation rate).

BM		Tool rotation rate (rpm)	Traverse speed (mm min^{-1})
6082	LRR-FSP	200	50
	HRR-FSP	1500	50
5086	LRR-FSP	400	100
	HRR-FSP	1200	100
7075	LRR-FSP	400	50
	HRR-FSP	800	50
7055	LRR-FSP	300	100
	HRR-FSP	1500	100
7055-0.25Sc	LRR-FSP	300	100
	HRR-FSP	1500	100

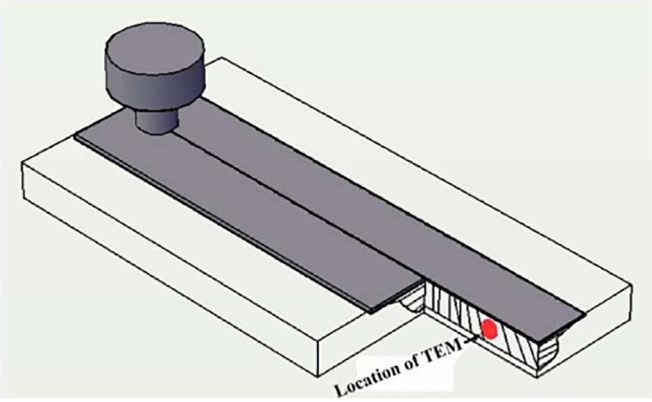

Fig. 1. Schematic illustration of the sampling location of TEM analysis.

2. Experimental

The raw materials were AA 5086-H112 (4.1 Mg, 0.45 Mn, 0.16 Fe and 0.1 Cr), AA 6082-T4 (1.16 Si, 0.77 Mg, 0.68 Mn and 0.27 Fe), AA 7075 (5.5 Zn, 2.4 Mg, 1.5 Cu and 0.13 Fe) after solution treatment (SS), AA 7055-SS (7.82 Zn, 2.24 Cu, 1.95 Mg and 0.16 Zr) and AA 7055-0.25Sc-T6 alloys. FSP was conducted at traverse speeds of 50 to 100 mm min^{-1} and tool rotation rates of 200 to 1500 rpm. The FSW parameters for each FSP sample are shown in Table 1.

The microstructures of the samples were examined by electron backscattered diffraction (EBSD) and transmission electron microscopy (TEM, JEM-2010). EBSD measurements were carried out by scanning electron microscopy (SEM, Hitachi S-3400N-II). A schematic illustration of the sampling location of TEM analysis is shown in Fig. 1. The films for TEM were prepared by grinding to a thickness of 50 μm, followed by thinning using a twinjet electropolishing device.

The damping capacity of the samples was characterized using specimens with dimensions of 1.2 mm × 4 mm × 25 mm. Damping tests were conducted by a dynamic mechanical analyzer (Q800, TA) in single-cantilever mode. Measurements were made at strain amplitudes (ε) of 7×10^{-5} to 2×10^{-1}, temperatures (T) of 40 to 360 °C with a heating rate of 5 °C/min and a constant frequency (f) of 1 Hz.

3. Results and Discussion

Fig. 2 shows the grain size distributions of the base metals (BMs) obtained by EBSD. The 5086 (Fig. 2a) and 7075 (Fig. 2c) BMs showed coarse equiaxed structures, while elongated grain structures were observed in the 6082 (Fig. 2b), 7055 (Fig. 2d) and 7055-0.25Sc (Fig. 2e) BMs.

Fig. 3 shows the grain size distributions of the FSP samples obtained by EBSD. The completely recrystallized grains with an equiaxed shape were observed in all the FSP samples. For the same alloy, the LRR-FSP sample exhibited finer grains than the HRR-FSP sample. Increasing the rotation rate enhanced the heat input during FSP and therefore led to the coarsening of recrystallized grains. The LRR-FSP 6082 alloy exhibited the smallest average grain size (AGS), which was as fine as 0.8 μm (Fig. 3c). The AGS of the HRR-FSP 5086 alloy was ~10.5 μm (Fig. 3b), larger than that of other FSP samples.

Fig. 4 shows the TEM images of the BMs. Some large phases containing Mg, Mn and Fe were observed in the 5086, 6082 and 7075 BMs (Fig. 4a–c). The 7055 and 7055-0.25Sc alloys after SS or T6 treatment

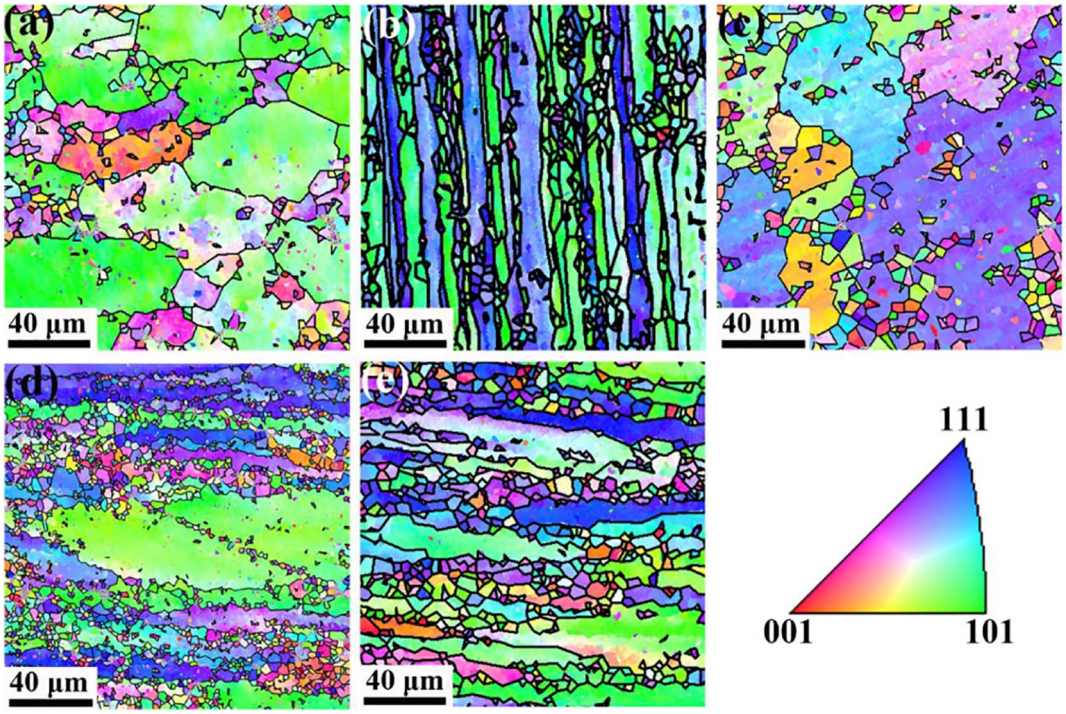

Fig. 2. EBSD maps showing grain structure of (a) 5086, (b) 6082, (c) 7075, (d) 7055, and (e) 7055-0.25Sc BMs.

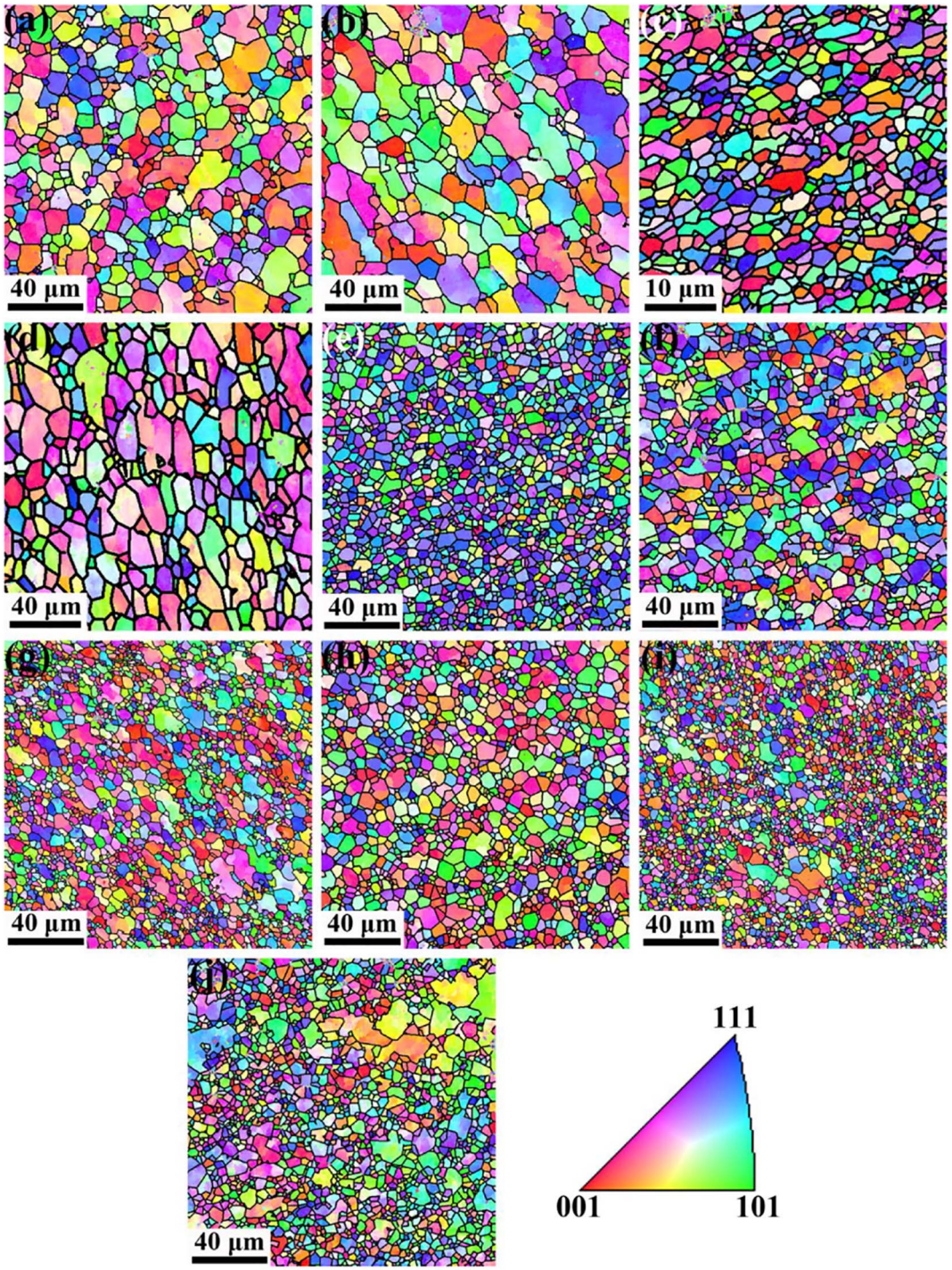

Fig. 3. EBSD maps showing grain structure of FSP (a, b) 5086, (c, d) 6082, (e, f) 7075, (g, h) 7055 and (i, j) 7055-0.25Sc alloys. (a, c, e, g, and i) LRR-FSP and (b, d, f, h and j) HRR-FSP samples.

exhibited much lower densities of large phases than other BMs due to the lower Mn and Fe, which with low solubility in Al lattice, contains (Fig. 4d and f). However the nanosized Al_3(Sc, Zr) particles were observed near the GBs of the 7055-0.25Sc alloys (Fig. 4e).

Fig. 5 shows the TEM images of the LRR-FSP samples. The phase transformation in the 5086 alloy (a non-age-hardened Al alloy) did not occur during FSP (Fig. 5a). However, the FSP resulted in the significant breakup of the particles and a more uniform distribution of particles in the matrix. Furthermore, the thermo-mechanical coupling effects also promoted the annihilation of dislocations in the 5086 BM.

For the age-hardened Al alloys (6082, 7075, 7055 and 7055-0.25Sc), the FSP samples exhibited a higher density and larger size of precipitates (Fig. 5b–e). Heat was generated from the severe friction between the tool and the workpiece during the plastic deformation of FSP or FSW, and a number of previous studies demonstrated that the temperature rise was sufficient to promote the precipitation and coarsening of the precipitates, and then the stable phases, which were incoherent with the Al matrix, were observed in the age-hardened Al alloys after FSP or FSW [12,15,20,21]. Thus, the β phase (Mg_2Si) precipitated in the LRR-FSP 6082 sample and the η phase (Zn_2Mg) precipitated in the LRR-FSP 7075, 7055 and 7055-0.25Sc samples.

Fig. 6 shows the strain amplitude dependent damping properties of

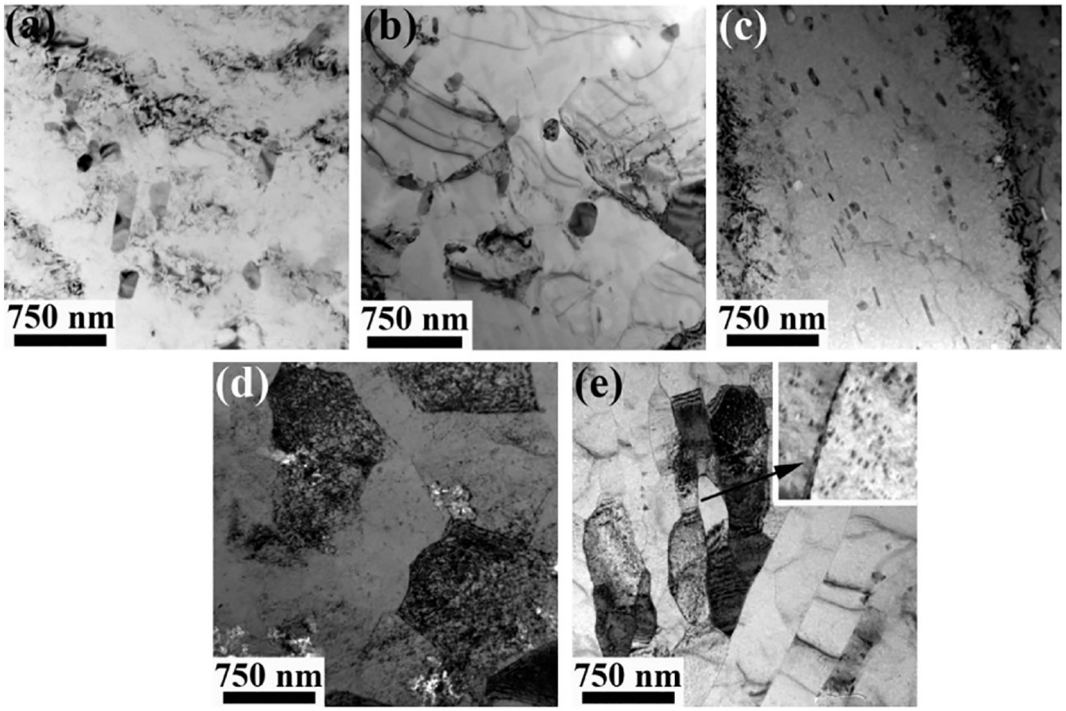

Fig. 4. TEM images of (a) 5086, (b) 6082, (c) 7075, (d) 7055 and (e) 7055-0.25Sc BMs. The insert in panel (e) shows the high density of Al3(Sc, Zr) particles located at the GB.

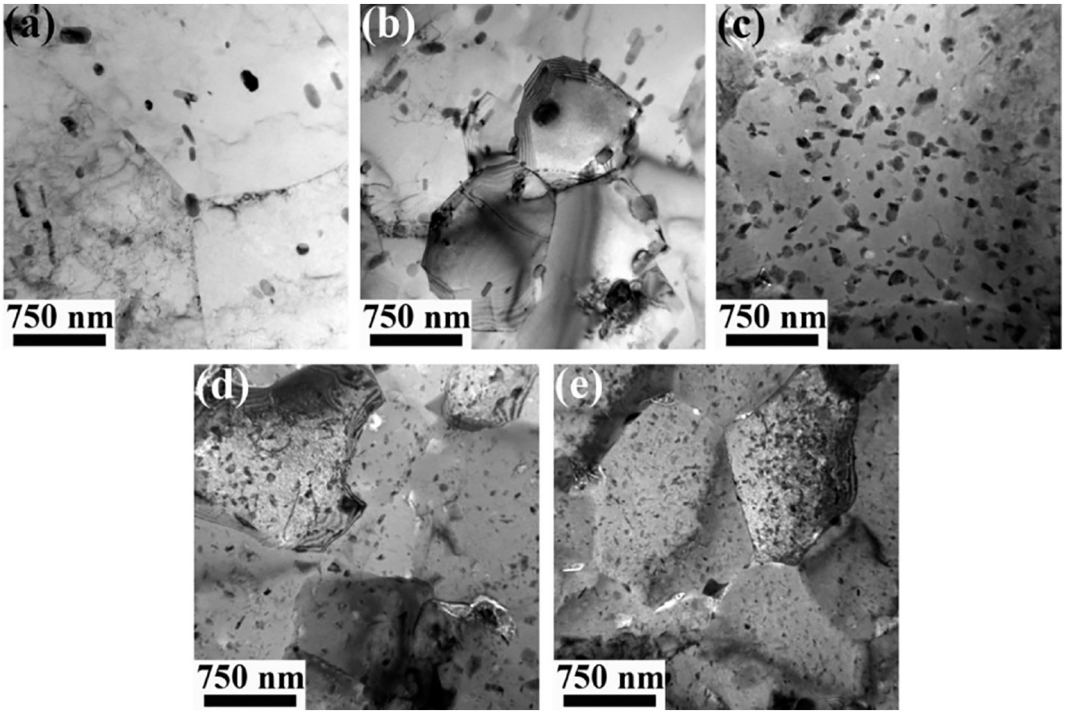

Fig. 5. TEM images of LRR-FSP (a) 5086, (b) 6082, (c) 7075, (d) 7055 and (e) 7055-0.25Sc.

the 5086, 6082 and 7075 BMs and their FSP samples. The room temperature damping capacities of the BMs and FSP samples were improved with increasing strain amplitude in the general trend due to that the movable dislocations broke away from the pinning points during high amplitude vibration [22].

FSP improved the damping capacities of the 6082 and 7075 alloys. This was attributed to the change of microstructures in those alloys during FSP. FSP promoted the formation of stable phases, and a large number of solute atoms were consumed during the precipitation process. The decreased number of solute atoms decreased the pinning points of movable dislocations during vibration. Furthermore, FSP also increased the density of incoherent phases. Similar to the Al matrix composites, which were high damping Al materials, more movable dislocations were generated near the particle-matrix interfaces in the FSP Al alloys during vibration. Both an enhanced movable dislocation number and weakened pinning effect improved the energy absorption properties of the FSP 6082 and 7075 samples, thereby significantly improving their room temperature damping capacities.

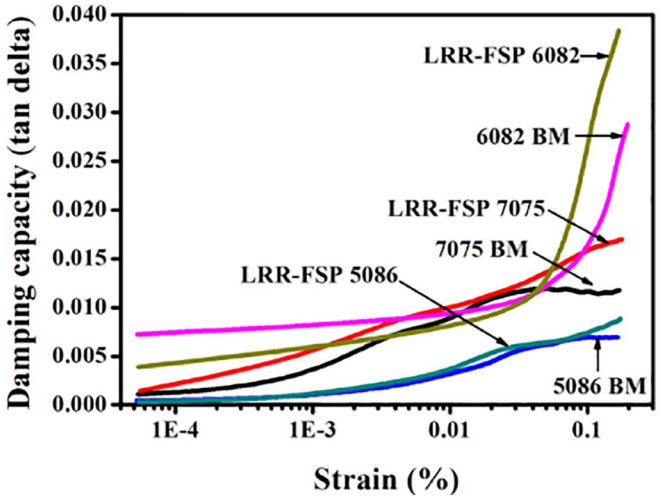

Fig. 6. Strain amplitude dependent damping capacities of BM and LRR-FSP samples.

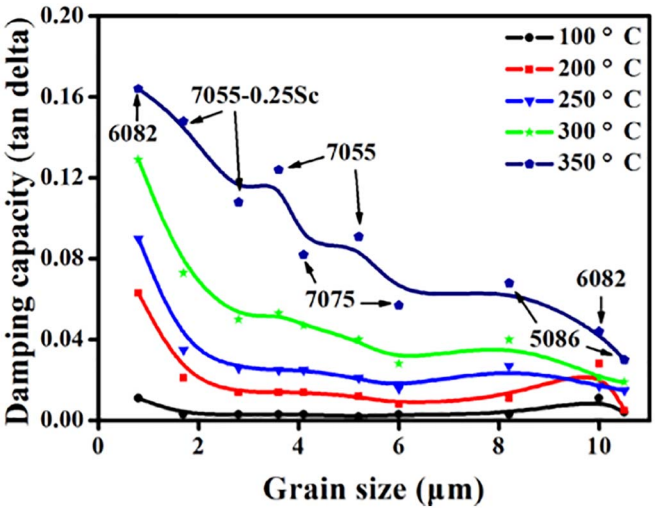

Fig. 8. Dependence of damping capacities on grain size of the FSP Al alloys.

FSP did not promote the precipitation in the non-age-hardened Al alloy. Thus, compared with the 5086 BM, the FSP 5086 sample did not exhibit significantly improved damping capacity. However, the higher density and uniform distribution of incoherent phase (Figs. 4a and 5a) promoted the generation of more movable dislocations during vibration, and therefore improved the damping capacity of the FSP 5086 sample slightly.

Fig. 7 shows the variation of damping capacities with temperature for the BM and LRR-FSP samples. The damping capacities of all samples were improved with increasing temperature due to the viscous flow at GBs converting mechanical energy into thermal energy as a result of internal friction at GBs [23].

The microstructure of the FSP samples was characterized by equiaxed grain structure, random grain misorientation distribution, predominant high angle GBs and a low density of dislocations (Fig. 3). This special microstructure always contributes to excellent GB sliding capacity and superplasticity above 250 °C [15–19]. Thus, for the same Al alloys, the FSP sample exhibited much higher high temperature damping capability than the BM.

The temperature of damping peaks at ~260 (Fig. 7a), 190 (Fig. 7b) and 200 °C (Fig. 7c) were observed in the curves for the LRR-FSP 5086, LRR-FSP 6082 and LRR-FSP 7 xxx samples, respectively. For the FSP samples, the damping peaks decreased with decreasing grain size (Fig. 3). Cai et al. [24] and Yang et al. [25] associated the damping peak in temperature range of 167 to 180 °C with the GB relaxation in the Al specimens with the structure of AGS lower than 100 nm. Therefore, the grain refinement could decrease the temperature of the damping peak,

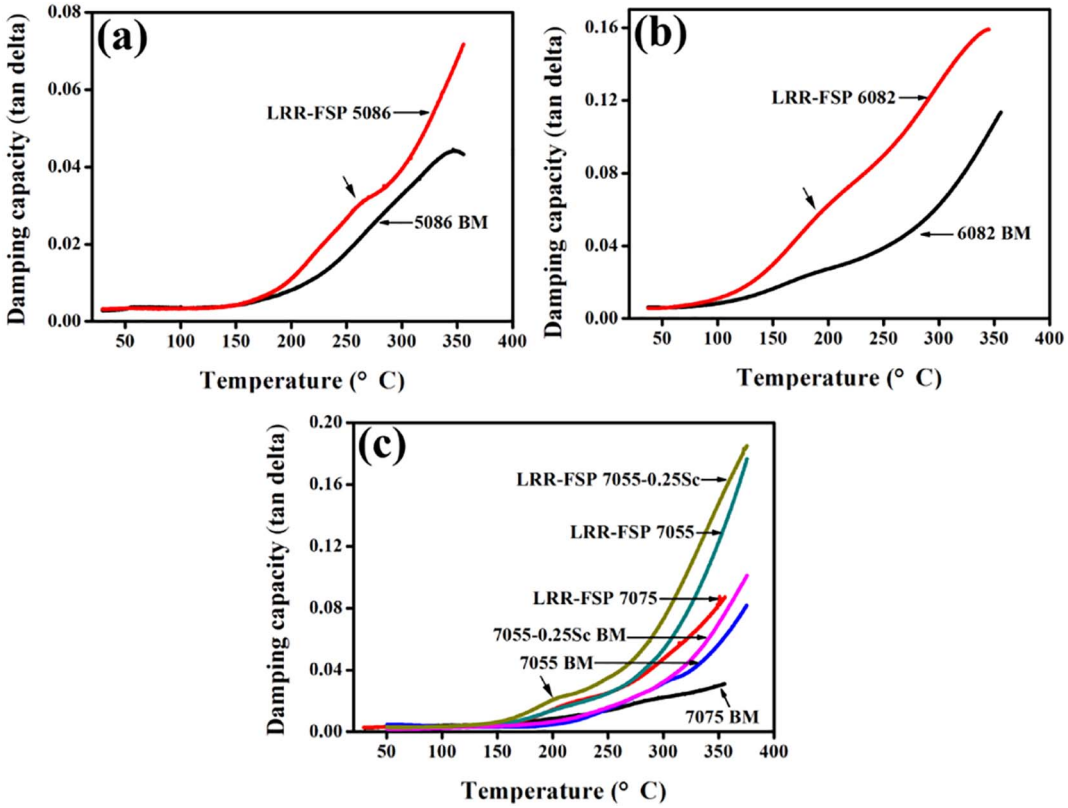

Fig. 7. Temperature dependent damping capacities of (a) 5086, (b) 6082 and (c) 7xxx alloys. The arrows denote the damping peaks of the LRR-FSP samples.

which induces the GB damping mechanism in Al alloys. This phenomenon is attributed to the grain refinement, which can decrease the GB sliding temperature [17].

Fig. 8 shows the dependence of damping capacities on the grain size of the FSP Al alloys. When the test temperature was lower than 250 °C, the internal friction value nearly did not change with the grain size.

Liu et al. [17] found that the GB sliding capacity of the FSP Al alloys at high temperature can be improved by the grain refinement. Thus, when the test temperature was higher than 250 °C, the internal friction value of the FSP samples decreased with increasing AGS, and the damping capacity of these samples did not depend on the alloy type. Thus, the LRR-FSP 6082 alloy exhibited the best high temperature damping capability, while the HRR-FSP 5086 alloy with the AGS being larger than 10 μm, showed the worst damping capability.

The LRR-FSP 7055-0.25Sc alloy exhibited higher increment in the internal friction with temperature than other FSP samples, when the temperature was higher than 260 °C (Fig. 8). The nanosized Al_3(Sc, Zr) precipitates can be obtained in the 7055 alloy after the Sc addition (Fig. 4e) and this phase can strongly pin the GBs during FSP and consequently promote grain refinement (Fig. 3). Furthermore, the Al_3(Sc, Zr) particles, which were located at the GBs in the LRR-FSP 7055-0.25Sc alloys can also strongly pin the GBs during damping test at high temperature, thereby preventing intense grain growth. The high thermal stability of the LRR-FSP 7055-0.25Sc alloy improved the high temperature damping capacity of this sample.

4. Conclusions

The damping capacity of both the age-hardened and non-age-hardened Al alloys at both room and high temperatures were simultaneously improved by FSP. This was attributed to the special microstructure characterized by an equiaxed grain structure, random misorientation grain distribution, predominant high angle GBs, low density of dislocations, low amount of solute atoms and uniform distribution and high density of incoherent phases. The temperature dependent damping capacities of the FSP samples can be improved by the grain refinement due to the enhanced GB sliding capacity. Furthermore, the GB pinning phase can also optimize the damping capacities of the FSP Al alloys at high temperature. This study suggests the potential of fabricating commercial Al alloys with excellent damping properties.

Acknowledgements

This work was funded by the National Natural Science Foundation of China (No. 51601045), Guangxi Natural Science Foundation (No. 2016GXNSFDA380028 and 2015GXNSFBA139238), and the Guangxi 'Bagui' Teams for Innovation and Research.

References

[1] Y.H. Zhao, X.Z. Liao, S. Cheng, E. Ma, Y.T. Zhu, Simultaneously increasing the ductility and strength of nanostructured alloys, Adv. Mater. 18 (2006) 2280–2283.
[2] D. Wang, Z.Y. Ma, Effect of pre-strain on microstructure and stress corrosion cracking of over-aged 7050 aluminum alloy, J. Alloys Compd. 469 (2009) 445–450.
[3] T. Hu, K. Ma, T.D. Topping, J.M. Schoenung, E.J. Lavernia, Precipitation phenomena in an ultrafine-grained Al alloy, Acta Mater. 61 (2013) 2163–2178.
[4] Y.J. Zhang, N.H. Ma, H.W. Wang, X.F. Li, Study on damping behavior of A356 alloy after grain refinement, Mater. Des. 29 (2008) 706–708.
[5] M.C. Gui, D.B. Wang, J.J. Wu, G.J. Yuan, C.G. Li, Deformation and damping behaviors of foamed Al-Si-SiCp composite, Mater. Sci. Eng. A 286 (2000) 282–288.
[6] J.P. Oliveira, J.F. Duarte, P. Inácio, N. Schell, R.M. Miranda, T.G. Santos, Production of Al/NiTi composites by friction stir welding assisted by electrical current, Mater. Des. 113 (2017) 311–318.
[7] H.J. Jiang, C.Y. Liu, B. Zhang, P. Xue, Z.Y. Ma, K. Luo, M.Z. Ma, R.P. Liu, Simultaneously improving mechanical properties and damping capacity of Al–Mg–Si alloy through friction stir processing, Mater. Charact. 131 (2017) 425–430.
[8] X.S. Hu, K. Wu, M.Y. Zheng, Effect of heat treatment on the stability of damping capacity in hypoeutectic Mg–Si alloy, Scr. Mater. 54 (2006) 1639–1643.
[9] C.D. Lee, Damping properties on age hardening of Al–7Si–0.3 Mg alloy during T6 treatment, Mater. Sci. Eng. A 394 (2005) 112–116.
[10] B.H. Luo, Z.H. Bai, Y.Q. Xie, The effects of trace Sc and Zr on microstructure and internal friction of Zn–Al eutectoid alloy, Mater. Sci. Eng. A 370 (2004) 172–176.
[11] W.M. Thomas, E.D. Nicholas, J.C. Needham, M.G. Murch, P. Templesmith, Dawes CJ GB Patent Application (1991) No. 9125978.8.
[12] R.S. Mishra, Z.Y. Ma, Friction stir welding and processing, Mater. Sci. Eng. R 50 (2005) 1–78.
[13] K. Zhao, Z.Y. Liu, B.L. Xiao, Z.Y. Ma, Friction stir welding of carbon nanotubes reinforced Al-Cu-Mg alloy composite plates, J. Mater. Sci. Technol. 33 (2017) 1004–1008.
[14] B.B. Wang, F.F. Chen, F. Liu, W.G. Wang, P. Xue, Z.Y. Ma, Enhanced mechanical properties of friction stir welded 5083Al-H19 joints with additional water cooling, J. Mater. Sci. Technol. 33 (2017) 1009–1014.
[15] I. Charit, R.S. Mishra, Low temperature superplasticity in a friction-stir-processed ultrafine grained Al–Zn–Mg–Sc alloy, Acta Mater. 53 (2005) 4211–4223.
[16] F.C. Liu, Z.Y. Ma, F.C. Zhang, High strain rate superplasticity in a micro-grained Al–Mg–Sc alloy with predominant high angle grain boundaries, J. Mater. Sci. Technol. 28 (2012) 1025–1030.
[17] F.C. Liu, Z.Y. Ma, L.Q. Chen, Low-temperature superplasticity of Al–Mg–Sc alloy produced by friction stir processing, Scr. Mater. 60 (2009) 968–971.
[18] Z.Y. Ma, F.C. Liu, R.S. Mishra, Superplastic deformation mechanism of an ultrafine-grained aluminum alloy produced by friction stir processing, Acta Mater. 58 (2010) 4693–4704.
[19] Z.Y. Ma, S.R. Sharma, R.S. Mishra, Effect of multiple-pass friction stir processing on microstructure and tensile properties of a cast aluminum–silicon alloy, Scr. Mater. 54 (2006) 1623–1626.
[20] Z.Y. Ma, Friction stir processing technology: a review, Metall. Mater. Trans. A 39 (2008) 642–658.
[21] Y. Chen, C.Y. Liu, B. Zhang, Z.Y. Ma, W.B. Zhou, H.J. Jiang, H.F. Huang, L.L. Wei, Effects of friction stir processing and minor Sc addition on the microstructure, mechanical properties, and damping capacity of 7055 Al alloy, Mater. Charact. 135 (2018) 25–31.
[22] H.J. Jiang, C.Y. Liu, Z.Y. Ma, X. Zhang, L. Yu, M.Z. Ma, R.P. Liu, Fabrication of Al–35Zn alloys with excellent damping capacity and mechanical properties, J. Alloys Compd. 722 (2017) 138–144.
[23] H. Watanabe, T. Mukai, M. Sugioka, K. Ishikawa, Elastic and damping properties from room temperature to 673 K in an AZ31 magnesium alloy, Scr. Mater. 51 (2004) 291–295.
[24] B. Cai, Q.P. Kong, P. Cui, H.T. Cong, X.K. Sun, Internal friction of nanocrystalline aluminum prepared by plasma evaporation and compaction, Scr. Mater. 44 (2001) 1043–1048.
[25] Z.Q. Yang, J. Chen, L.L. He, H.T. Cong, H.Q. Ye, Microstructure and grain boundary relaxation in ultrafine-grained Al/Al oxide composites, Acta Mater. 57 (2009) 3633–3644.